*AgriEngineering*

MDPI

*Technical Note*

# LeafLaminaMap: Exploring Leaf Color Patterns Using RGB Color Indices

**Péter Bodor-Pesti [1], Lien Le Phuong Nguyen [2,*], Thanh Ba Nguyen [3], Mai Sao Dam [3], Dóra Taranyi [1] and László Baranyai [2]**

[1] Department of Viticulture, Institute for Viticulture and Oenology, Buda Campus, Hungarian University of Agriculture and Life Sciences, 29-43 Villányi St., H-1118 Budapest, Hungary; bodor-pesti.peter@uni-mate.hu (P.B.-P.); taranyi.dora.agnes@uni-mate.hu (D.T.)
[2] Institute of Food Science and Technology, Hungarian University of Agriculture and Life Sciences, 35-43 Vil-lányi St., H-1118 Budapest, Hungary; baranyai.laszlo@uni-mate.hu
[3] Institute of Biotechnology and Food Technology, Industrial University of Ho Chi Minh City, Ho Chi Minh 700000, Vietnam; thanhngba@iuh.edu.vn (T.B.N.); damsaomai@iuh.edu.vn (M.S.D.)
* Correspondence: nguyen.le.phuong.lien@uni-mate.hu

**Abstract:** The color of the plant leaves is a major concern in many areas of agriculture. Pigmentation and its pattern provide the possibility to distinguish genotypes and a basis for annual crop management practices. For example, the nutrient and water status of plants is reflected in the chlorophyll content of leaves that are strongly linked to the lamina coloration. Pests and diseases (virus or bacterial infections) also cause symptoms on the foliage. These symptoms induced by biotic and abiotic stressors often have a specific pattern, which allows for their prediction based on remote sensing. In this report, an RGB (red, green and blue) image processing system is presented to determine leaf lamina color variability based on RGB-based color indices. LeafLaminaMap was developed in Scilab with the Image Processing and Computer Vision toolbox, and the code is available freely at GitHub. The software uses RGB images to visualize 29 color indices and the R, G and B values on the lamina, as well as to calculate the statistical parameters. In this case study, symptomatic (senescence, fungal infection, etc.) and healthy grapevine (*Vitis vinifera* L.) leaves were collected, digitalized and analyzed with the LeafLaminaMap software according to the mean, standard deviation, contrast, energy and entropy of each channel (R, G and B) and color index. As an output for each original image in the sample set, the program generates 32 images, where each pixel is constructed using index values calculated from the RGB values of the corresponding pixel in the original image. These generated images can subsequently be used to help the end-user identify locally occurring symptoms that may not be visible in the original RGB image. The statistical evaluation of the samples showed significant differences in the color pattern between the healthy and symptomatic samples. According to the F value of the ANOVA analysis, energy and entropy had the largest difference between the healthy and symptomatic samples. Linear discriminant analysis (LDA) and support vector machine (SVM) analysis provided a perfect recognition in calibration and confirmed that energy and entropy have the strongest discriminative power between the healthy and symptomatic samples. The case study showed that the LeafLaminaMap software is an effective environment for the leaf lamina color pattern analysis; moreover, the results underline that energy and entropy are valuable features and could be more effective than the mean and standard deviation of the color properties.

**Keywords:** lamina; color variability; vegetation index; RGB pattern; energy; entropy

check for updates

Academic Editor: Zhengjun Qiu

Received: 30 December 2024
Revised: 19 January 2025
Accepted: 3 February 2025
Published: 6 February 2025

**Citation:** Bodor-Pesti, P.; Nguyen, L.L.P.; Nguyen, T.B.; Dam, M.S.; Taranyi, D.; Baranyai, L. LeafLaminaMap: Exploring Leaf Color Patterns Using RGB Color Indices. *AgriEngineering* **2025**, *7*, 39. https://doi.org/10.3390/agriengineering7020039

**Copyright:** © 2025 by the authors. Licensee MDPI, Basel, Switzerland. This article is an open access article distributed under the terms and conditions of the Creative Commons Attribution (CC BY) license (https://creativecommons.org/licenses/by/4.0/).

## 1. Introduction

Individual leaf coloration provides important information in agriculture, forestry and horticulture industries as well as in the food industry. The concentration of the pigments, particularly the chlorophyll, xanthophyll, carotenes, anthocyanin and betalains, indicate the nutrient status, signaling environmental stress and fungal, bacterial or viral infection and senescence [1–4]. In addition, color is important in the consumer perception of fresh produce such as leafy vegetables [5,6]. In the case of urban trees and ornamental plants, the color of the foliage is also important as it gives esthetic value [7]. Leaf pigmentation in a natural, unstressed environment is uniform, meaning that lamina contains pigments approximately in the same concentration as the whole organ. There are exceptions such as variegations induced by numerous factors, for example, differential gene expression, leaf blisters, viruses and genetic mosaicism. These phenomena have specific patterns on one single organ or between the organs [8,9].

In biotic- or abiotic-stress conditions, leaves may change coloration. Nutrient deficiencies, for example, have typical pattern. Uneven nitrogen availability causes smaller leaf size and light green coloration [10]. Magnesium deficiency could show different symptoms where the main symptom is chlorotic yellowing [11] that occurs between the veins; while the veins themselves remain green, other symptoms could include necrotic spots and purplish or reddish hues. Potassium deficiency causes similar symptoms such as yellowing that starts at the serrations of older leaves, while the centers may remain green. Fungal infections also have a significant effect on leaf coloration. Downy mildew, for example, causes "oil spots" [12]; powdery mildew is characterized by white spots [13]; black rot has typical brownish-reddish spots with dark edges [14], while ESCA causes irregular light green coloration, chlorotic symptoms [15], followed by the typical "tiger-stripe" pattern [16].

Vegetation indices (VIs) are dimensionless values that reflect the qualitative and quantitative properties of the biomass. Since the introduction of the first ratio-based indices: "Ratio Vegetation Index" (RVI = R/NIR) and "Vegetation Index Number" (VIN = NIR/R) in 1972, several further indices were developed; for example, the most known one is NDVI [17]. Vegetation indices are valuable tools for detecting growth decline, nutrient deficiencies, water stress, frost damage or biotic environmental stressors. Approaching the issue from a sensor perspective, both RGB-based multispectral and hyperspectral imaging provide valuable data for VI calculation. Multispectral and hyperspectral sensors have the advantage of including the NIR band, providing deeper information about the vegetation, while the RGB-based indices are cheaper as an ordinary digital camera or a smartphone could be applied as a sensor device [18,19]. Beside the cost effectiveness, the use of RGB sensors has many more benefits. The images reflect the visible range of the spectrum, which makes it easy to use. The resolution is high enough for the detailed evaluation of the images. With certain settings (sRGB), the data format is standardized and compatible with many image-analysis software. Additionally, the RGB sensors have a fast capture time and require less computational power with simpler algorithms to evaluate. Of course, there are also disadvantages and limitations to using RGB data. For one, only a limited part of the spectrum can be evaluated, and several wavelengths are excluded from the observation that may be useful for understanding physiological processes. This limitation was partly solved with the use of vegetation indices that provide more specific information than the original RGB image. Another disadvantage is that it provides less data and therefore does not always allow for complex analysis.

RGB-based vegetation and color indices proved to be useful in many sectors of agriculture such as grass research [20,21] and horticulture, particularly for tomatoes [22], potatoes [23], cherries [24] and grapevines [25]. Sánchez-Sastre et al. [26] showed that there are several indices derived from the visible bands that have high correlation with the chlorophyll content; moreover, de Carvalho and Nunes [27] showed that smartphone-based RGB image analysis is appropriate for the prediction of chlorophyll and carotenoid contents in vegetable oils.

VIs are mainly used in areal image analysis from satellites, UAVs or drones, while on-the-go and stationary sensors are also available. In the former cases, resolution largely determines the level of details in the images and the conclusions that can be drawn from them. In the initial phase of the monitoring, the Landsat-4 and 5 provided 30 m spatial sampling [28]. Later on, this resolution was improved. Korznikov et al. [29], for example, obtained the images in their study from the GeoEye-1 satellite system with 0.46 m/pixel resolution. If these resolutions are not enough, UAV or proximal sensing solutions could provide better, even millimeter-scale, resolutions. For example, flatbed scanners are widely applied in morphological characterization [30,31], as these devices are cost effective, user friendly and provide valuable RGB information in high resolution. According to the settings, flatbed scanners deliver images from 300 to 1200 dpi, meaning 0.00717 $mm^2$/pixel and 0.000448 $mm^2$/pixel, respectively.

In most studies, VI is calculated at the vegetation, plantation, canopy, or plant level, while the individual leaf color-index pattern until now was not in the front of image analysis experiments. Therefore, the main goal of this study is to introduce a methodology for individual leaf investigation based on RGB-based color and vegetation indices. Additionally, statistical parameters and their classification methods are to be compared by utilizing surface VI maps. Upon the successful application of the recently developed LeafLaminaMap software, it is shared as an open-source measurement tool.

## 2. Materials and Methods

### 2.1. Plant Material and Digitalization

The plant material was collected from a commercial vineyard in Tata 'Látó-hegy' (Neszmély wine region, Tata, Hungary). The leaf sample set comprised two subsample groups. The first sample set consisted of healthy leaves from the middle third of several shoots without any visible deficiency or infection symptoms of the grapevine (*Vitis vinifera* L.) cultivar 'Hárslevelű', collected between the berry set in veraison 2024 from the NW and SE side (n = 10 leaves per side) of the canopy from SW-NE-oriented rows (GPS coordinates: 47.658294, 18.281226). The second sample set consisted of leaves from the following grapevine (*Vitis vinifera* L.) cultivars 'Kékfrankos', 'Pinot noir', Cserszegi fűszeres' and 'Leányka'. These samples were collected at the end of October 2024 from various locations to provide large intra- and inter-sample color variability caused by senescence and different pests and diseases.

Samples were stored in plastic bags for approximately 2 h and digitized with a Canon Pixma MG3650S flatbed scanner (Canon, Tokyo, Japan) using a resolution of 300 dpi and an sRGB color profile.

### 2.2. Color and Vegetation Indices

In this study, raw RGB data were utilized based on 29 RGB-based color and vegetation indices (Table 1) [26,32–34]. Many of these indices are considered as good indicators of leaf chlorophyll concentration [26,32]. Each color channel (R, G and B) and the calculated vegetation indices are evaluated utilizing the mean, standard deviation, contrast, energy and entropy of the leaf lamina pixels.

**Table 1.** Color and vegetation indices involved in the study.

| Index | Formula |
|---|---|
| Red chromaticity | $R/(R + G + B)$ |
| Green chromaticity | $G/(R + G + B)$ |
| Blue chromaticity | $B/(R + G + B)$ |
| RMG (Difference between red and green) | $R - G$ |
| RMB (Difference between red and blue) | $R - B$ |
| GMB (Difference between green and blue) | $G - B$ |
| NRGVI (Normalized red-green difference index) | $(R - G)/(R + G)$ |
| NRBVI (Normalized red-blue difference index) | $(R - B)/(R + B)$ |
| NGBVI (Normalized green-blue difference index) | $(G - B)/(G + B)$ |
| NGRVI (Normalized green-red difference index) | $(G - R)/(G + R)$ |
| NBRVI (Normalized blue-red difference index) | $(B - R)/(B + R)$ |
| NBGVI (Normalized blue-green difference index) | $(B - G)/(B + G)$ |
| WI (Woebbecke index) | $(G - B)/(R - G)$ |
| BI (Brightness index) | $((R^2 + B^2 + G^2)/3)^{1/2}$ |
| RGCh (Red-green chromaticity) | $(R - G)/(R + G + B)$ |
| RBCh (Red-blue chromaticity) | $(R - B)/(R + G + B)$ |
| GBCh (Green-blue chromaticity) | $(G - B)/(R + G + B)$ |
| GRCh (Green-red chromaticity) | $(G - R)/(R + G + B)$ |
| BRCh (Blue-red chromaticity) | $(B - R)/(R + G + B)$ |
| BGCh (Blue-green chromaticity) | $(B - G)/(R + G + B)$ |
| MGRVI (Modified green-red vegetation index) | $(G^2 - R^2)/(G^2 + R^2)$ |
| RGRI (Red-green ratio index) | $R/G$ |
| BGRI (Blue-green ratio index) | $B/G$ |
| GLI (Green leaf index) or VDVI (Visible band-difference vegetation index) | $(2G - R - B)/(2G + R + B)$ |
| VARI (Visible atmospherically resistance index) | $(G - R)/(G + R - B)$ |
| ExR (Excess red vegetation index) | $(1.4 \times R - G)/(R + G + B)$ |
| ExB (Excess blue vegetation index) | $(1.4 \times B - G)/(R + G + B)$ |
| ExG (Excess green vegetation index) | $(2 \times G - R - B)/(R + G + B)$ |
| ExGR (Excess green minus excess red) | $ExG - ExR$ |
| Red intensity | $R$ |
| Green intensity | $G$ |
| Blue intensity | $B$ |

### *2.3. Statistical Analysis*

The mean, standard deviation, contrast, energy and entropy of the samples for each color index and color band were calculated using the LeafLaminaMap (version 1.0, Baranyai and Bodor-Pesti, Hungary) software. During the statistical evaluation, ANOVA was carried out for each color index and their statistical parameters for the factor of 2 subsets: symptomatic and healthy grapevine leaves (n = 20 + 20). Linear discriminant analysis (LDA) and support vector machine (SVM) analysis were used to distinguish symptomatic and healthy leaves. The classification was evaluated via 10-fold cross validation with 80% teaching and 20% validation samples. Statistical analysis was performed using the R software (version 4.4.1, R Foundation for Statistical Computing, Vienna, Austria) and RStudio (version 2024.09.1+394, Posit Software PBC, Boston, MA, USA). Pearson correlation was calculated, and the matrix was illustrated with the PAST software (version 4.17c) [35].

### *2.4. Software*

The software of LeafLaminaMap (version 1.0) was made using the free software of Scilab (version 2024.1.0, Dassault Systèmes, Vélizy-Villacoublay, France) and the Image Processing and Computer Vision toolbox (IPCV version 4.5.0). The source code is available freely at GitHub (https://github.com/lbaranyai/Scilab/tree/main/lamina_map) (accessed on 4 February 2025) as a Scilab M file. It is not a compiled binary but a script ran by Scilab (using the "exec" command). The software offers a graphical user interface

with buttons and a list of color indices to facilitate rapid measurements. Functions are available to load scanned pictures, capture a new one with an available camera, save the selected color index map and analyze all color indices in batch. Results are displayed on the user interface for calculated parameters of the current color index, while the list of calculated values for all indices is automatically saved in a structured ASCII text file. This file format is used to offer easy import to any data analysis software. Leaves are segmented on the picture first, assuming a white background. The leaf surface is transformed to the selected color index on which statistical features are calculated. The parameters of mean, standard deviation, contrast (Equation (1)), energy (Equation (2)) and entropy (Equation (3)) are computed. In the following equations, $i$ is the intensity, and $P(i)$ is the probability of intensity $i$ on the surface with $\Sigma P(i) = 1$. The listed equations yield contrast ($C$), energy ($E$) and entropy ($S$).

$$C = \sum i^2 P(i) \quad (1)$$

$$E = \sum P(i)^2 \quad (2)$$

$$S = -\sum P(i) \log_{10} P(i) \quad (3)$$

## 3. Results

### *3.1. Color Analyis with the LeafLaminaMap Software*

LeafLaminaMap handles JPEG format images. After loading the images into the program, the original RGB image is displayed in the window (Figure 1). The user has the possibility to choose from the color indices. Then, the mean, standard deviation, contrast, energy and entropy data are provided by the software at the organ level. Simultaneously, the program visualizes the leaf pattern derived from the pixels set indexed according to the RGB values computed from the original image (Figure 2). The button "Save image" gives the possibility to save the current VI map of the leaf. Clicking on the button "Scan and Save" runs all the VI transformations for the RGB image and saves the mean, standard deviation, contrast, energy and entropy of the leaf lamina pixels in a CSV format. Generated VI maps for a selected example picture are available as Supplementary Material S1.

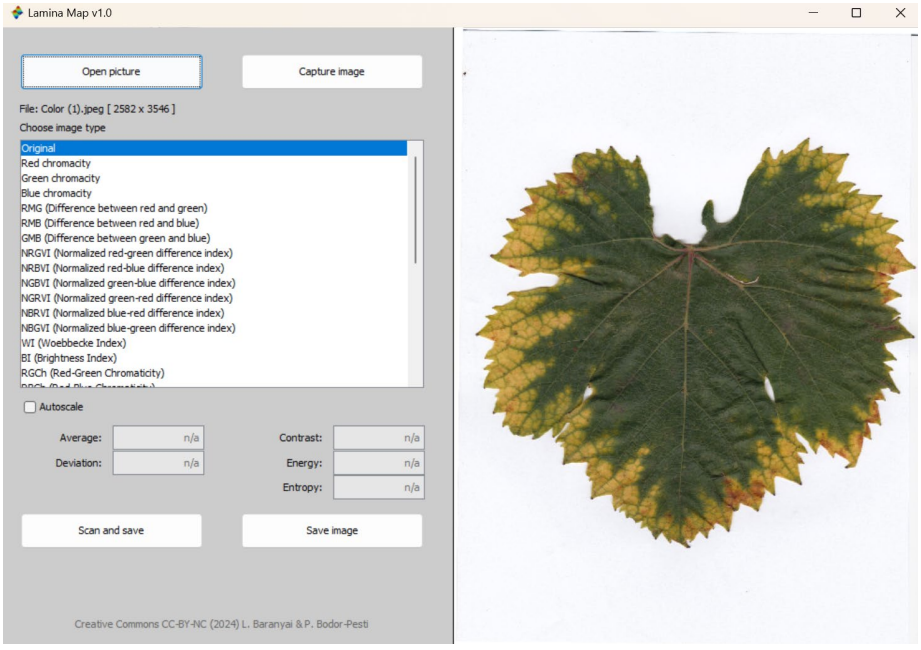



**Figure 1.** User interface of the LeafLaminaMap software.

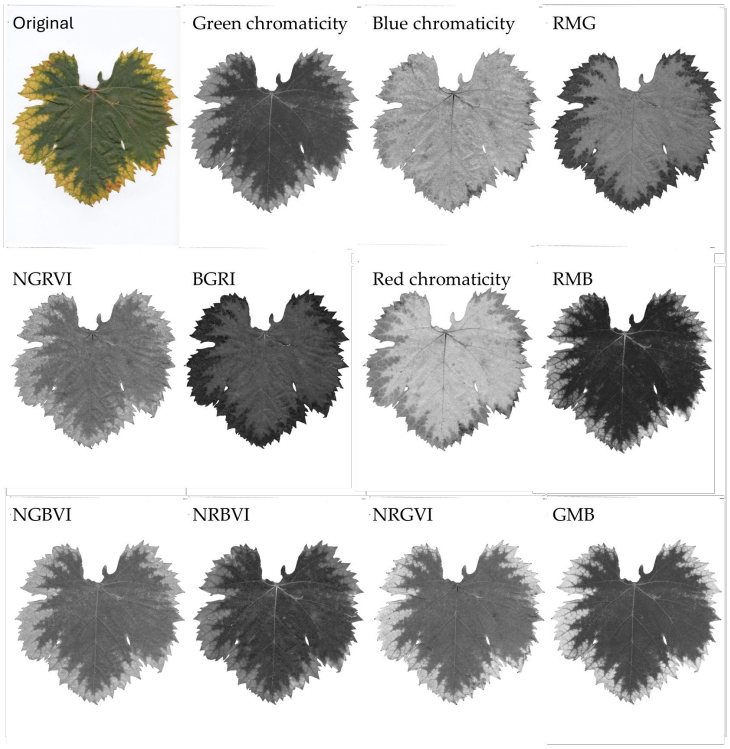



**Figure 2.** Original picture and 11 color indices calculated using the LeafLaminaMap software.

### *3.2. Colorimetic Evaluation*

#### 3.2.1. Mean and Standard Deviation of the Color Indices

Mean values of all color indices were calculated based on the individual pixel values and subjected to ANOVA between the healthy and symptomatic samples (Table 2). Except for NGBVI, NBGVI, GBCh, BGCh, BGRI and ExB, all measured indices showed a significant difference (Table 2). The highest F values (F = 58.23, $p < 0.01$) were obtained in the case of NRBVI and NBRVI, meaning that these two vegetation indices (based on the red-blue color edge) had the largest difference between the symptomatic and healthy leaves. The standard deviation showed less variability between the two sample sets as less indices obtained a significant difference. The following indices showed no significant difference in standard deviation: green chromacity, blue chromacity, NGBVI, NBGVI, BI, GBCh, BGCh, BGRI, GLI, ExG and ExB. The standard deviation achieved the largest difference between the healthy and symptomatic leaves in the case of red chromaticity, with F = 90.46 ($p < 0.01$).

**Table 2.** Effect of stress on leaf color indices according to ANOVA F values.

| Color Index | Mean | St.dev. | Contrast | Energy | Entropy |
|---|---|---|---|---|---|
| Red chromacity | 58.11 * | 90.46 * | 54.11 * | 433.89 * | 840.79 * |
| Green chromacity | 19.59 * | 0.49 | 14.70 * | 541.21 * | 394.89 * |
| Blue chromacity | 29.69 * | 0.28 | 25.89 * | 41.85 * | 62.74 * |
| RMG | 27.53 * | 69.10 * | 5.55 + | 110.78 * | 172.90 * |
| RMB | 43.19 * | 46.54 * | 21.98 * | 42.88 * | 76.59 * |
| GMB | 10.36 * | 28.61 * | 17.78 * | 10.05 * | 17.88 * |
| NRGVI | 45.48 * | 29.79 * | 2.52 | 615.66 * | 610.49 * |
| NRBVI | 58.23 * | 9.56 * | 35.30 * | 71.52 * | 116.00 * |
| NGBVI | 1.52 | 1.34 | 8.06 * | 33.04 * | 48.41 * |

**Table 2.** *Cont.*

| Color Index | Mean | St.dev. | Contrast | Energy | Entropy |
|---|---|---|---|---|---|
| NGRVI | 45.48 * | 29.79 * | 6.34 + | 604.62 * | 604.52 * |
| NBRVI | 58.23 * | 9.56 * | 33.80 * | 71.44 * | 115.31 * |
| NBGVI | 1.52 | 1.34 | 5.21 + | 32.56 * | 48.08 * |
| Woebbecke index | 45.62 * | 18.02 * | 12.70 * | 37.10 * | 53.11 * |
| Brightness index | 31.30 * | 2.65 | 24.14 * | 0.05 | 1.57 |
| RGCh | 44.27 * | 31.45 * | 2.38 | 907.45 * | 777.73 * |
| RBCh | 57.42 * | 29.45 * | 33.54 * | 123.68 * | 291.67 * |
| GBCh | 0.02 | 2.55 | 4.02 | 107.75 * | 161.17 * |
| GRCh | 44.27 * | 31.45 * | 6.98 + | 904.02 * | 771.21 * |
| BRCh | 57.42 * | 29.45 * | 30.92 * | 123.19 * | 291.29 * |
| BGCh | 0.02 | 2.55 | 0.11 | 107.18 * | 160.82 * |
| MGRVI | 50.65 * | 32.32 * | 6.17 + | 285.85 * | 260.47 * |
| RGRI | 27.45 * | 18.20 * | 23.76 * | 188.72 * | 453.15 * |
| BGRI | 0.51 | 1.65 | 0.12 | 14.35 * | 26.22 * |
| GLI | 18.10 * | 2.39 | 0.00 | 376.33 * | 322.05 * |
| VARI | 47.07 * | 25.68 * | 6.76 + | 49.55 * | 176.58 * |
| ExR | 47.67 * | 44.80 * | 22.54 * | 825.24 * | 844.31 * |
| ExG | 19.59 * | 0.49 | 0.83 | 514.64 * | 380.40 * |
| ExB | 1.46 | 2.74 | 8.81 * | 91.69 * | 148.86 * |
| ExGR | 32.66 * | 7.57 * | 6.98 + | 696.10 * | 551.28 * |
| Red intensity | 39.62 * | 14.20 * | 27.15 * | 4.40 + | 12.66 * |
| Green intensity | 16.17 * | 5.04 + | 15.43 * | 1.65 | 5.52 + |
| Blue intensity | 7.07 + | 5.54 + | 4.45 + | 28.72 * | 23.71 * |

* $p < 0.01$, + $p < 0.05$.

#### 3.2.2. Contrast, Energy and Entropy of the Color Indices

According to the ANOVA F values, the parameter entropy showed the highest sensitivity with the maximum average F value, followed by the parameter energy (Table 2). Their average F values were more than 10-fold higher than those of the mean, standard deviation and contrast. On the other hand, the energy of the red-green chromacity (RGCh) achieved the maximum F value, with F = 907.45 ($p < 0.01$). Contrast showed high variability among the samples as seven indices did not provide a significant response: NRGVI, RGCh, GBCh, BGCh, BGRI, GLI and ExG. Energy was a sensitive statistical parameter as 93.75% of the evaluated VIs obtained a significant difference between the sample sets, except for BI and green intensity. The most sensitive descriptor was entropy, as BI was the only index without a significant difference.

#### 3.2.3. Correlation of the Color and Vegetation Indices

Pearson's correlation was evaluated for the mean value of the investigated vegetation indices (Figure 3). It was found that some of the indices showed 100% correlation due to the calculation using the formula for ExG and green chromacity (correlation coefficient = 1; $p < 0.05$), BGCh and GBCh, BRCh and RBCh, GRCh and RGCh, NGRVI and NGBVI, NBRVI and NRBVI, and NBGVI and NRGVI (correlation coefficient = −1; $p < 0.05$).

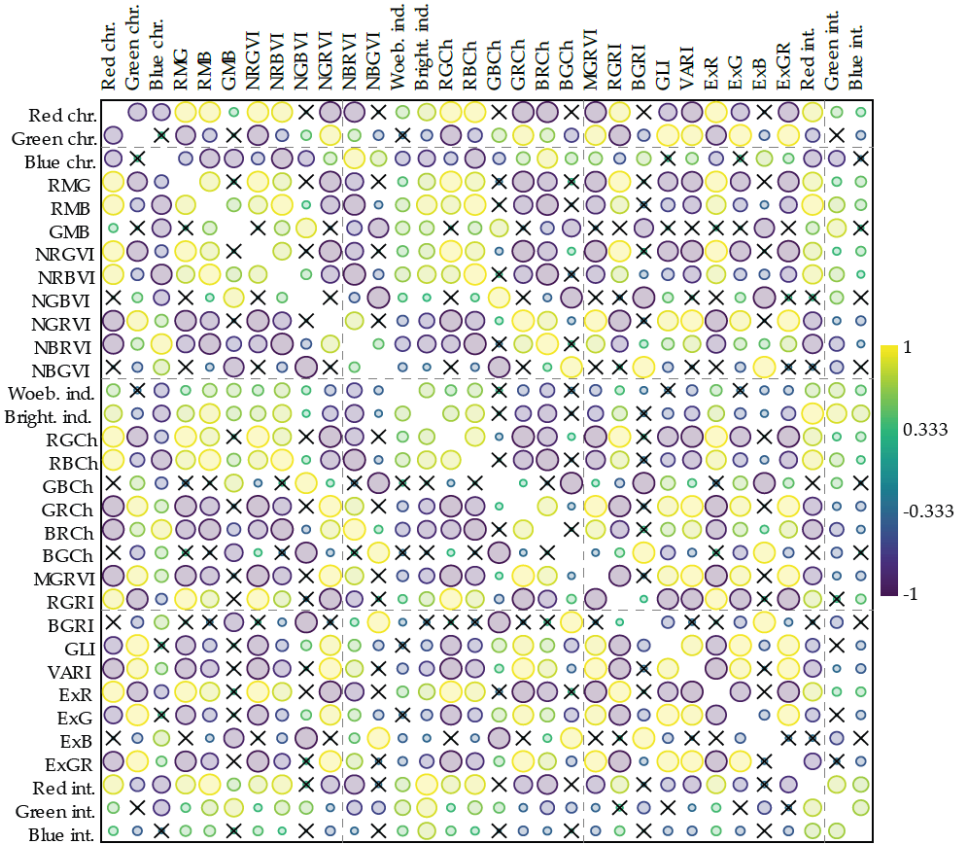



**Figure 3.** Pearson's correlation of the investigated color properties. Cross refers to $p > 0.05$.

### *3.3. Classification of Leaf Samples*

The classification results based on the listed color indices are summarized in Table 3. The LDA and SVM with linear kernel achieved perfect recognition in calibration. Cross-validation results decreased compared to that of calibration, except for the statistical parameters of energy and entropy. They were the strongest features and performed with the highest accuracy (100%). Considering the 10-fold cross-validation results of all statistical parameters, both LDA and SVM (with linear and radial kernel) can be recommended for the detection of symptomatic leaves.

**Table 3.** Classification accuracy (%) of calibration and cross-validation on leaf samples.

| Feature | LDA | SVM Linear | SVM Radial | SVM Polynomial | SVM Sigmoid |
|---|---|---|---|---|---|
| | | | Calibration | | |
| Average | 100 | 100 | 95.00 | 82.50 | 92.50 |
| Deviation | 95.00 | 100 | 100 | 85.00 | 98.75 |
| Contrast | 91.20 | 100 | 95.00 | 72.50 | 92.80 |
| Energy | 100 | 100 | 100 | 100 | 100 |
| Entropy | 100 | 100 | 100 | 100 | 100 |
| | | | Validation | | |
| Average | 100 | 93.75 | 93.75 | 82.50 | 88.75 |
| Deviation | 83.75 | 93.75 | 97.50 | 81.25 | 97.50 |
| Contrast | 90.00 | 93.75 | 92.50 | 72.50 | 87.50 |
| Energy | 100 | 100 | 100 | 100 | 100 |
| Entropy | 100 | 100 | 100 | 100 | 100 |

## 4. Discussion

Plant's spectral reflectance can be monitored at various scales. The analysis of large geographical areas could be useful in land use studies, geomorphology, forestry or even

arable crop production [9,36–38]. This level of monitoring could give detailed information about the vegetation or plantation structure. The more detailed approaches available using drones allow for the characterization of smaller plant communities and individual medium or small-sized plants or even organs, which can be further enhanced by sensors placed in the plantations or on the go. If the investigations do not require in situ conditions, there are many simple and cost-effective ways to digitize and analyze the RGB range of the reflected spectrum. Studies reported in recent decades showed that digital image analysis provides high and valuable resolution, especially for the samples digitalized with flatbed scanners [39–42]. Beside morphology and morphometry, one of the many research directions is color analysis where scanned images provide valuable results [43,44]. Considering the field experiments, scanning wands (portable handheld scanners) can be used as well by putting a white board behind the leaves and scanning manually. Such a portable scanner can transfer images to the computer via a USB connection or WiFi or by storing them on a memory card. In this study, a Canon Pixma Mg3650S flatbed scanner was applied at a resolution of 300 dpi and an sRGB-standardized color profile that provides consistent color reproduction and compatibility with the different manufacturers. Sunlight can disturb measurements and affect color information [45]. Therefore, cameras should be used in controlled environments like a light tent, or reference color cards can help in the standardization of color information [46–48]. Due to the leaf's morphology, primarily flatbed or handheld scanners are recommended for high resolution data acquisition. Scanners are more robust and prevent light scattering into the sensor effectively. The applied sRGB color profile is standardized, making the results comparable with those obtained using other devices [39–44].

Vegetation indices are widely applied for environmental research, and many software platforms are available to calculate the indices from the RGB or multispectral images such as QGIS [49], ArcGIS [50] or in Python [51]. These solutions give the freedom to calculate as many indices as the user wants and what the original information allows. On the other hand, technical skills are essential to operate these platforms which may discourage the user. For this reason, easy-to-use solutions have great importance. LeafLaminaMap has been designed with the ease of use and a user-friendly interface as the primary considerations. The software uses simple RGB images to calculate color and vegetation indices that proved to be valuable in plant physiological monitoring [26,52]. The data provided by the LeafLaminaMap software would be applicable for various purposes based on linear discriminant analysis (LDA), neural network (NN), support vector machines (SVMs) or random forest (RF) as these methods are powerful for the classification and identification of genotypes or for the detection of pests and diseases [53–56]. The limitation of the software is that only the data are provided, but no analysis is performed. Since many factors can contribute to color change, the software can be considered as a general-purpose measurement tool presently. On the other hand, the open-source code enables easy integration to any framework or other software packages. In this study, the collected data were evaluated using ANOVA, LDA and SVM to find differences between symptomatic and healthy (asymptomatic) grapevine leaf samples. Results showed that color indices and their statistical features (mean, standard deviation, contrast, energy and entropy) significantly differ between the two sample sets. In most studies, color indices are evaluated according to the mean values that represent the objects or area subjected for investigation [26]. This way of data evaluation has undoubted advantages, and further features give deeper insights to the variability of the pigmentation. Lhermitte et al. [57] introduced the importance of entropy in a computer vision and RGB-based classification based on advanced statistical methods. Damayanti et al. [58] investigated RGB images and identified nine color features that had a high correlation with the chlorophyll content of *Vernonia amygdalina*. Among these features,

the energy and entropy of the b* from L*a*b* were listed. Later, Sekharamantry et al. [59] showed that entropy is an important feature during the evaluation of leaf images of medical plants. Among other color features, Padmavathi and Deepa [60] utilized energy to detect citrus plant diseases. In our study, both entropy and energy of the investigated color and vegetation indices obtained high F values and classification accuracy. This underlines the effectiveness of these features in the comparison of symptomatic and healthy leaf samples.

## 5. Conclusions

In this study, an open-source software is presented and provides a user-friendly easy-to-use platform for the RGB color index and its pattern evaluation of the leaf lamina. The script was shown to work using the free software of Scilab and the IPCV toolbox. As a case study, LeafLaminaMap (version 1.0) was tested on healthy and symptomatic grapevine leaves at the same time. The proposed method is general and can be applied to any plant species. Multivariate classification methods (LDA and SVM) were able to distinguish symptomatic and healthy leaves, especially by utilizing energy and entropy. It was found that all color features provided valuable information, while energy and entropy were the most effective statistical parameters in the differentiation of the two sample sets. The introduced solution could be applied for various purposes such as deficiency detection, or evaluation of the effect of environmental stress or biotic infections. The software is a general-purpose measurement tool, providing statistical parameters on color indices. The open-source code allows for the easy integration of the method in other software tools. Since calculated parameters describe spatial variability, the presented technique might be useful in a wide range of application such as remote sensing. For instance, conducting RGB image analysis from UAV platforms such as drones to describe the variability of larger agricultural areas. It is also possible to implement the method of on-the-go monitoring, for example, with a webcam, and receive information about the biomass of plantations, soil covering, ripeness level evaluation or even weed research. Since smartphones have an integrated RGB camera, the vegetation indices included in the LeafLaminaMap software are easy to implement into an application, providing a valuable tool for growers to perform fast monitoring.

**Supplementary Materials:** The following supporting information can be downloaded at: https://www.mdpi.com/article/10.3390/agriengineering7020039/s1: Example picture and generated vegetation index maps.

**Author Contributions:** Conceptualization, L.B. and P.B.-P.; methodology, L.B. and P.B.-P.; software, L.B.; investigation, P.B.-P., and D.T.; resources, L.B. and P.B.-P.; data curation, L.B., P.B.-P. and L.L.P.N.; writing—original draft preparation, L.B., P.B.-P., L.L.P.N., D.T., T.B.N. and M.S.D.; writing—review and editing, L.B., P.B.-P., L.L.P.N., D.T., T.B.N. and M.S.D.; visualization, L.B. and P.B.-P. All authors have read and agreed to the published version of the manuscript.

**Funding:** This research received no external funding.

**Data Availability Statement:** Software code, sample images and data are available at GitHub. https://github.com/lbaranyai/Scilab/tree/main/lamina_map (accessed on 4 February 2025).

**Conflicts of Interest:** The authors declare no conflicts of interest.

## References

1. Talebzadeh, F.; Valeo, C. Evaluating the effects of environmental stress on leaf chlorophyll content as an index for tree health. In *IOP Conference Series: Earth and Environmental Science*; IOP Publishing: Bristol, UK, 2022; Volume 1006. [CrossRef]
2. Turnbull, C. Changes in Pigment Accumulation as Indicators of Physical Stress in Eucalyptus pauciflora. *Field Stud. Ecol.* **2019**, *2*, 10. Available online: https://studentjournals.anu.edu.au/index.php/fse/article/view/220 (accessed on 18 January 2025).

3. Zhou, Y.; Karl, T.; Lewis, D.H.; McGhie, T.K.; Arathoon, S.; Davies, K.M.; Ryan, K.G.; Gould, K.S.; Schwinn, K.E. Production of betacyanins in transgenic *Nicotiana tabacum* increases tolerance to salinity. *Front. Plant Sci.* **2021**, *12*, 653147. [CrossRef] [PubMed]
4. Lázár, J.; Bisztray, G.D. Virus and virus-like diseases of grapevine in Hungary. *Int. J. Hortic. Sci.* **2011**, *17*, 25–36. [CrossRef]
5. Saba, A.; Moneta, E.; Peparaio, M.; Sinesio, F.; Vassallo, M.; Paoletti, F. Towards a multi-dimensional concept of vegetable freshness from the consumer's perspective. *Food Qual. Prefer.* **2018**, *66*, 1–12. [CrossRef]
6. Fouladkhah, A.; Bunning, M.; Stone, M.; Stushnoff, C.; Stonaker, F.; Kendall, P. Consumer hedonic evaluation of eight fresh specialty leafy greens and their relationship to instrumental quality attributes and indicators of secondary metabolites. *J. Sens. Stud.* **2011**, *26*, 175–183. [CrossRef]
7. Liang, D.; Huang, G. Influence of Urban Tree Traits on Their Ecosystem Services: A Literature Review. *Land* **2023**, *12*, 1699. [CrossRef]
8. Marcotrigiano, M. Chimeras and variegation: Patterns of deceit. *HortScience* **1997**, *32*, 773–784. [CrossRef]
9. Zhang, H.; Feng, S.; Wu, D.; Zhao, C.; Liu, X.; Zhou, Y.; Zheng, S. Hyperspectral Image Classification on Large-Scale Agricultural Crops: The Heilongjiang Benchmark Dataset, Validation Procedure, and Baseline Results. *Remote Sens.* **2024**, *16*, 478. [CrossRef]
10. Sun, Y.; Tong, C.; He, S.; Wang, K.; Chen, L. Identification of nitrogen, phosphorus, and potassium deficiencies based on temporal dynamics of leaf morphology and color. *Sustainability* **2018**, *10*, 762. [CrossRef]
11. Wiwart, M.; Fordoński, G.; Żuk-Gołaszewska, K.; Suchowilska, E. Early diagnostics of macronutrient deficiencies in three legume species by color image analysis. *Comput. Electron. Agric.* **2009**, *65*, 125–132. [CrossRef]
12. Abdelghafour, F.; Keresztes, B.; Germain, C.; Da Costa, J.P. In field detection of downy mildew symptoms with proximal color imaging. *Sensors* **2020**, *20*, 4380. [CrossRef] [PubMed]
13. Rivera-Romero, C.A.; Palacios-Hernández, E.R.; Vite-Chávez, O.; Reyes-Portillo, I.A. Early-Stage Identification of Powdery Mildew Levels for Cucurbit Plants in Open-Field Conditions Based on Texture Descriptors. *Inventions* **2024**, *9*, 8. [CrossRef]
14. Szabó, M.; Csikász-Krizsics, A.; Dula, T.; Farkas, E.; Roznik, D.; Kozma, P.; Deák, T. Black rot of grapes (*Guignardia bidwellii*)—A comprehensive overview. *Horticulturae* **2023**, *9*, 130. [CrossRef]
15. Letousey, P.; Baillieul, F.; Perrot, G.; Rabenoelina, F.; Boulay, M.; Vaillant-Gaveau, N.; Fontaine, F. Early events prior to visual symptoms in the apoplectic form of grapevine esca disease. *Phytopathology* **2010**, *100*, 424–431. [CrossRef]
16. Calzarano, F.; Pagnani, G.; Pisante, M.; Bellocci, M.; Cillo, G.; Metruccio, E.G.; Di Marco, S. Factors Involved on Tiger-Stripe Foliar Symptom Expression of Esca of Grapevine. *Plants* **2021**, *10*, 1041, *Decline of Mediterranean Fruit Crops and Forests Associated with Fungal Trunk Pathogens 117*. [CrossRef]
17. Bannari, A.; Morin, D.; Bonn, F.; Huete, A. A review of vegetation indices. *Remote Sens. Rev.* **1995**, *13*, 95–120. [CrossRef]
18. Ponti, M.P. Segmentation of low-cost remote sensing images combining vegetation indices and mean shift. *IEEE Geosci. Remote Sens. Lett.* **2012**, *10*, 67–70. [CrossRef]
19. Tao, M.; Ma, X.; Huang, X.; Liu, C.; Deng, R.; Liang, K.; Qi, L. Smartphone-based detection of leaf color levels in rice plants. *Comput. Electron. Agric.* **2020**, *173*, 105431. [CrossRef]
20. Barbosa, B.D.S.; Ferraz, G.A.S.; Gonçalves, L.M.; Marin, D.B.; Maciel, D.T.; Ferraz, P.F.P.; Rossi, G. RGB vegetation indices applied to grass monitoring: A qualitative analysis. *Agron. Res.* **2019**, *17*, 349–357. [CrossRef]
21. Kazemi, F.; Ghanbari Parmehr, E. Evaluation of RGB vegetation indices derived from UAV images for rice crop growth monitoring. *ISPRS Ann. Photogramm. Remote Sens. Spat. Inf. Sci.* **2023**, *10*, 385–390. [CrossRef]
22. Elmetwalli, A.H.; Derbala, A.; Alsudays, I.M.; Al-Shahari, E.A.; Elhosary, M.; Elsayed, S.; Al-Shuraym, L.A.; Moghanm, F.S.; Elsherbiny, O. Machine learning-driven assessment of biochemical qualities in tomato and mandarin using RGB and hyperspectral sensors as nondestructive technologies. *PLoS ONE* **2024**, *19*, e0308826. [CrossRef] [PubMed]
23. Li, B.; Xu, X.; Han, J.; Zhang, L.; Bian, C.; Jin, L.; Liu, J. The estimation of crop emergence in potatoes by UAV RGB imagery. *Plant Methods* **2019**, *15*, 15. [CrossRef] [PubMed]
24. Morgan, G.R.; Stevenson, L. Unoccupied-Aerial-Systems-Based Biophysical Analysis of Montmorency Cherry Orchards: A Comparative Study. *Drones* **2024**, *8*, 494. [CrossRef]
25. Ilniyaz, O.; Kurban, A.; Du, Q. Leaf area index estimation of pergola-trained vineyards in arid regions based on UAV RGB and multispectral data using machine learning methods. *Remote Sens.* **2022**, *14*, 415. [CrossRef]
26. Sánchez-Sastre, L.F.; Alte da Veiga, N.M.; Ruiz-Potosme, N.M.; Carrión-Prieto, P.; Marcos-Robles, J.L.; Navas-Gracia, L.M.; Martín-Ramos, P. Assessment of RGB vegetation indices to estimate chlorophyll content in sugar beet leaves in the final cultivation stage. *AgriEngineering* **2020**, *2*, 128–149. [CrossRef]
27. de Carvalho, T.C.L.; Nunes, C.A. Smartphone-based method for the determination of chlorophyll and carotenoid contents in olive and avocado oils: An approach with calibration transfer. *J. Food Compos. Anal.* **2021**, *104*, 104164. [CrossRef]
28. Pahlevan, N.; Balasubramanian, S.V.; Sarkar, S.; Franz, B.A. Toward long-term aquatic science products from heritage Landsat missions. *Remote Sens.* **2018**, *10*, 1337. [CrossRef]

29. Korznikov, K.A.; Kislov, D.E.; Altman, J.; Doležal, J.; Vozmishcheva, A.S.; Krestov, P.V. Using U-Net-like deep convolutional neural networks for precise tree recognition in very high resolution RGB (red, green, blue) satellite images. *Forests* **2021**, *12*, 66. [CrossRef]
30. Viscosi, V.; Cardini, A. Leaf morphology, taxonomy and geometric morphometrics: A simplified protocol for beginners. *PLoS ONE* **2011**, *6*, e25630. [CrossRef]
31. Bylesjö, M.; Segura, V.; Soolanayakanahally, R.Y.; Rae, A.M.; Trygg, J.; Gustafsson, P.; Jansson, S.; Street, N.R. LAMINA: A tool for rapid quantification of leaf size and shape parameters. *BMC Plant Biol.* **2008**, *8*, 82. [CrossRef]
32. Cheng, L.; Zhu, X.; Gao, L.; Li, C.; Wang, L.; Zhao, G.; Jiang, Y. Estimation of chlorophyll content in apple leaves based on RGB model using digital camera. *Acta Hortic. Sin.* **2017**, *44*, 381.
33. Kawashima, S.; Nakatani, M. An algorithm for estimating chlorophyll content in leaves using a video camera. *Ann. Bot.* **1998**, *81*, 49–54. [CrossRef]
34. Biró, L.; Kozma-Bognár, V.; Berke, J. Comparison of RGB Indices used for Vegetation Studies based on Structured Similarity Index (SSIM). *J. Plant Sci. Phytopathol.* **2024**, *8*, 007–012. [CrossRef]
35. Hammer, Ø.; Harper, D.A. Past: Paleontological statistics software package for education and data analysis. *Palaeontol. Electron.* **2001**, *4*, 1.
36. Dou, P.; Shen, H.; Huang, C.; Li, Z.; Mao, Y.; Li, X. Large-scale land use/land cover extraction from Landsat imagery using feature relationships matrix based deep-shallow learning. *Int. J. Appl. Earth Obs. Geoinf.* **2024**, *129*, 103866. [CrossRef]
37. Xu, H.; Cheng, W.; Wang, B.; Song, K.; Zhang, Y.; Wang, R.; Bao, A. Effects of Geomorphic Spatial Differentiation on Vegetation Distribution Based on Remote Sensing and Geomorphic Regionalization. *Remote Sens.* **2024**, *16*, 1062. [CrossRef]
38. Cushman, K.C. *Remote Sensing of Forest Structure and Dynamics in the Barro Colorado Nature Monument*; Smithsonian Institution Scholarly Press: Washington, DC, USA, 2024. [CrossRef]
39. Brewer, M.T.; Lang, L.; Fujimura, K.; Dujmovic, N.; Gray, S.; van der Knaap, E. Development of a controlled vocabulary and software application to analyze fruit shape variation in tomato and other plant species. *Plant Physiol.* **2006**, *141*, 15–25. [CrossRef]
40. Gonzalo, M.J.; Brewer, M.T.; Anderson, C.; Sullivan, D.; Gray, S.; van der Knaap, E. Tomato fruit shape analysis using morphometric and morphology attributes implemented in Tomato Analyzer software program. *J. Am. Soc. Hortic. Sci.* **2009**, *134*, 77–87. [CrossRef]
41. Králík, M.; Klíma, O.; Urbanová, P.; Polcerová, L.; Čuta, M. Morphometric Sex Estimation from the Hip Bone by Means of the HIP 1.1 Software. In *Shape in Medical Imaging: International Workshop, ShapeMI 2018, Held in Conjunction with MICCAI 2018, Granada, Spain*; Springer: Cham, Switzerland, 2018; Volume 11167, p. 78.
42. Johnson, M.T.; Bertrand, J.A.; Turcotte, M.M. Precision and accuracy in quantifying herbivory. *Ecol. Entomol.* **2016**, *41*, 112–121. [CrossRef]
43. Darrigues, A.; Hall, J.; van der Knaap, E.; Francis, D.M.; Dujmovic, N.; Gray, S. Tomato analyzer-color test: A new tool for efficient digital phenotyping. *J. Am. Soc. Hortic. Sci.* **2008**, *133*, 579–586. [CrossRef]
44. Brabec, D.; Grothe, S.; Perez-Fajardo, M.; Pordesimo, L.; Yeater, K. Potential of a flatbed scanner for evaluation of flour samples for dark specks and flour color. *Cereal Chem.* **2024**, *101*, 508–517. [CrossRef]
45. Baek, S.H.; Park, K.H.; Jeon, J.S.; Kwak, T.Y. A novel method for calibration of digital soil images captured under irregular lighting conditions. *Sensors* **2022**, *23*, 296. [CrossRef] [PubMed]
46. Chizk, T.M.; Lee, J.A.; Clark, J.R.; Worthington, M.L. ShinyFruit: Interactive fruit phenotyping software and its application in blackberry. *Front. Plant Sci.* **2023**, *14*, 1182819. [CrossRef] [PubMed]
47. Clohessy, J.W.; Pauli, D.; Kreher, K.M.; Buckler, E.S.; Armstrong, P.R.; Wu, T.; Hoekenga, O.A.; Jannink, J.L.; Sorrells, M.E.; Gore, M.A. A Low-Cost Automated System for High-Throughput Phenotyping of Single Oat Seeds. *Plant Phenome J.* **2018**, *1*, 1–13. [CrossRef]
48. Bodor-Pesti, P.; Taranyi, D.; Nyitrainé Sárdy, D.Á.; Le Phuong Nguyen, L.; Baranyai, L. Correlation of the Grapevine (*Vitis vinifera* L.) Leaf Chlorophyll Concentration with RGB Color Indices. *Horticulturae* **2023**, *9*, 899. [CrossRef]
49. QGIS Association. Free and Open Source Geographic Information System. In *QGIS Geographic Information System*; QGIS Association: Gossau, Switzerland, 2015.
50. ESRI. *ArcGIS Desktop: Release 10*; Environmental Systems Research Institute: Redlands, CA, USA, 2011.
51. Van Rossum, G.; Drake, F.L., Jr. *Python Reference Manual*; Centrum Voor Wiskunde en Informatica Amsterdam: Amsterdam, Netherlands, 1995.
52. Domínguez-Manzano, J.; Monago-Maraña, O.; Muñoz de la Peña, A.; Durán-Merás, I. Monitoring of chlorophylls during the maturation stage of plums by multivariate calibration of RGB data from digital images. *Chemosensors* **2022**, *11*, 9. [CrossRef]
53. Panahi, B.; Mohammadi, S.A.; Doulati-Baneh, H. Characterization of Iranian grapevine cultivars using machine learning models. *Proc. Natl. Acad. Sci. India Sect. B Biol. Sci.* **2020**, *90*, 615–621. [CrossRef]
54. Patil, S.P.; Zambre, R.S. Classification of cotton leaf spot disease using support vector machine. *Int. J. Eng. Res.* **2014**, *3*, 1511–1514.

55. Pydipati, R.; Burks, T.F.; Lee, W.S. Identification of citrus disease using color texture features and discriminant analysis. *Comput. Electron. Agric.* **2006**, *52*, 49–59. [CrossRef]
56. Nyitrainé Sárdy, Á.D.; Ladányi, M.; Varga, Z.; Szövényi, Á.P.; Matolcsi, R. The effect of grapevine variety and wine region on the primer parameters of wine based on 1H NMR-spectroscopy and machine learning methods. *Diversity* **2022**, *14*, 74. [CrossRef]
57. Lhermitte, E.; Hilal, M.; Furlong, R.; O'brien, V.; Humeau-Heurtier, A. Deep Learning and Entropy-Based Texture Features for Color Image Classification. *Entropy* **2022**, *24*, 1577. [CrossRef] [PubMed]
58. Damayanti, R.; Riza, D.F.A.; Putranto, A.W.; Nainggolan, R.J. Vernonia Amygdalina Chlorophyll Content Prediction by Feature Texture Analysis of Leaf Color. In *IOP Conference Series: Earth and Environmental Science*; IOP Publishing: Bristol, UK, 2021; Volume 757, No. 1, p. 012026. [CrossRef]
59. Sekharamantry, P.K.; Rao, M.S.; Srinivas, Y.; Uriti, A. PSR-LeafNet: A Deep Learning Framework for Identifying Medicinal Plant Leaves Using Support Vector Machines. *Big Data Cogn. Comput.* **2024**, *8*, 176. [CrossRef]
60. Padmavathi, K.; Deepa, C. Swarm Intelligence Based Detection of Citrus Plant Diseases and Their Severity Level. *Int. J. Innov. Technol. Explor. Eng.* **2020**, *3*, 428–433. [CrossRef]


**Disclaimer/Publisher's Note:** The statements, opinions and data contained in all publications are solely those of the individual author(s) and contributor(s) and not of MDPI and/or the editor(s). MDPI and/or the editor(s) disclaim responsibility for any injury to people or property resulting from any ideas, methods, instructions or products referred to in the content.